IMS-CID-IMS-MS to Dissociate
Non-covalent Complexes for Enhanced Resolution of Tryptic Peptides

Brian Bohrer
C500: Introduction to Research
1st Year Report
Submitted April 21, 2006

Research Conducted Under Supervision of:
Prof. David Clemmer

Introduction:

Background on IMS

A fairly mature and straightforward technique, ion mobility spectrometry (IMS), has recently experienced renewed interest in the detection of drugs and explosives[1], complex mixture analysis[2], and structural studies of metal clusters[3] and biomolecules[4]. The main feature of a modern ion mobility spectrometer is the drift tube, which contains a buffer gas (typically helium or other chemically inert gas) at pressures ranging from ~0.001 to 1 atmosphere, depending on the instrument. The sample of interest must be ionized before analysis, which is typically done by electron impact (EI), pulsed laser vaporization[5], matrix-assisted laser desorption/ioniziation (MALDI)[6], or electrospray ionization (ESI) techniques[7]. Upon entering the drift tube, the analyte ions are accelerated by an applied electric field. Collisions with the buffer gas molecules decelerate the analyte ions, causing them to travel at a constant drift velocity for the majority of their trajectory through the drift tube. Drift velocities are obviously functions of the electric field strength and are therefore normalized by taking the ratio of these two quantities. This ratio is referred to as the ion's mobility, K, and is given by

$$K = \frac{\upsilon_D}{E} \qquad (1)$$

where K is mobility, υ_D is drift velocity, and E is electric field strength[8]. As charge on the ion increases, so will its drift velocity. Therefore, families of charge states can readily be visualized in IMS data. Within a given charge state, larger or more elongated ions will experience more collisions than compact ions. This indicates an inverse relationship between mobility and collision cross-section. As a result, biomolecules with the same

charge and primary structure may potentially be resolved based solely on their conformation.

If the applied electric field is sufficiently weak, the ions will move slowly relative to their thermal motion. This condition is referred to as the low-field limit, and if exceeded, the analyte ions will be thermally excited and will deform or interconvert between conformations during the separation. Therefore, experiments aiming to preserve and study structure must be performed under low-field limit conditions. Data from these experiments can be used to find collision cross-sections of structures with the relation

$$\Omega = \frac{(18\pi)^{1/2}}{16}\frac{ze}{(k_B T)^{1/2}}\left[\frac{1}{m_i}+\frac{1}{m_B}\right]^{1/2}\frac{t_D E}{L}\frac{760}{P}\frac{T}{273.2}\frac{1}{N} \qquad (2)$$

where Ω is the collision cross-section, z is the charge state of the ion, e is the fundamental charge of the electron, and m_i and m_B refer to the mass of the ion and buffer gas respectively. P and T represent the pressure and temperature, while k_B refers to the Boltzmann constant, L refers to the length of the drift tube, and N states the number density of the buffer gas[8]. The collision cross-section of a particular biomolecule can also be modeled and theoretically calculated for various energy-minimized structures[9]. Comparison between these two quantities enables the assignment of structure to an observed mobility peak; provided that one and only one calculated collision cross-section is within experimental agreement with the data.

As a separation technique, it is well known that IMS experiences an inherent correlation between size and mass. While intuition may readily lead one to such a conclusion, the exact mathematical relationship can be found in Eqn (2) above. This connection becomes especially apparent as IMS commonly utilizes mass spectrometry

(MS) as a detector. Therefore, it is not surprising to find that IMS-MS analysis of complex mixtures still produces many unresolved peaks. Additional degrees of separation must be incorporated if one wishes to sufficiently isolate and identify each component of complex biological mixtures, as is the case in the field of proteomics. To achieve this, Lee *et al.* added a liquid chromatography (LC) stage preceding the electrospray source of the IMS-MS instrument[10]. LC is a viable additional degree of separation because it separates components based on their affinities for the mobile and stationary phases. In other words, rather than size or mass, LC manipulates a chemical property.

An alternative chemical property to exploit in a separation involves the use of non-covalent adducts. By introducing molecules into the sample that will non-covalently bind to the analyte peptides, the mobilities of the components in the mixture can be altered to different extents, leading to resolution of originally overlapping ions. Because the formation of these complexes depends on chemical properties, the new degree of separation will be orthogonal to the drift-time and flight-time separations inherent to IMS-MS analysis. Incorporation of collision-induced dissociation (CID) region leads to IMS-CID-MS and enables the dissociation of the complex to retrieve the parent peptide[11]. Introduction of CID also changes the composition of the mixture due to the dissociation of adducts, as well as charge transfer events and fragmentation. Therefore, multidimensional experiments such as IMS-CID-IMS-MS would allow for the resolution of these newly formed components as they travel through the second drift region[12]. Ion funnels, the operation of which will be covered in the experimental section, can be used to divide a single drift tube into a two-dimensional separation instrument as well as supply the aforementioned CID region.

Background on crown ether project

The basis for this method was shown by Julian and Beauchamp when they demonstrated the ability of various crown ethers to form complexes around protonated lysine and arginine residues and N-termini of peptides[13]. These complexes are stable enough to survive the ESI process and are observable through mass spectrometry. Since then, others have studied this system using IMS-MS techniques. Colgate, Bramwell, and Creaser performed a study whereby the cross-sections of the sequence isomer tetrapeptides MFAR and MRFA were measured before and after the addition of various polyethers[14]. These included the crown ethers 12-crown-4 ether (12C4), 15-crown-5 ether (15C5), 18-crown-6 ether (18C6), and linear polyethers triglyme (T3G) and tetraglyme (T4G). The peptides were analyzed separately and formed dimers and trimers as well as complexes with one and two polyethers. Although the technique was not performed on a mixture, one can easily find the difference in mobility between two complexes (Table 1) and simulate the degree of separation that might be observed.

Hilderbrand and Clemmer have meanwhile applied this method to the actual analysis of peptide mixtures[15]. The study's most simple experiment examined three dipeptides, RA, KV, and LN, which are too similar in both mass and mobility to be resolved in a normal IMS-MS instrument. Upon the addition of crown ether, however, each dipeptide accepted a different number of adducts, resulting in significant differences in the mass-to-charge ratio and mobility of each complex. In a considerably more complex experiment, a combinatorial library of tripeptides containing lysine, arginine, or leucine at the first residue position (Fig 1) was treated with 18C6 (Fig. 2)[16]. Compared to the

original spectrum of untreated tripeptides, the resulting spectrum contained two additional clusters of peaks. These two clusters correlated to the single and double additions of 18C6 to the tripeptide library and were shifted to later drift times in the spectrum. A second experiment was then performed on this crown ether/tripeptide mixture, involving the removal of the crown ether from the complex at the end of the drift tube via CID. Once fragmented, the parent ions were observed, but at the same drift time as their respective complexes (Fig. 3)[16].

The first stage of my project involved showing reproducibility in the results of Hildebrand and Clemmer dipeptide study using a new, high-resolution IMS-CID-IMS-MS instrument. Next, the use of 18C6 as a shift reagent for IMS was applied to the analysis of a tryptic digest of cytochrome *c*. A tryptic digest seemed like an ideal sample because trypsin cleaves at lysine and arginine residues on a protein, ensuring every cleaved peptide contains at least one basic site in addition to its N-terminus. Therefore, crown ether should bind to every peptide, allowing the entire digest to be mobility-shifted.

Experimental:

Instrumentation

Figure 4 depicts the home-built, two-dimensional ion mobility-mass spectrometer used in these studies, the details of which have been covered more thoroughly elsewhere[12]. Ions are introduced into the drift tube via ESI-generated ion-injection and are pulled through the buffer gas (~3.0-3.3 Torr He) by a uniform electric field of 12 $V \cdot cm^{-1}$. To improve ion transmission, ion funnels have been placed at the entrance (F1), roughly at the center (F2), and at the exit (F3) of the drift tube which operate at fields of 11 $V \cdot cm^{-1}$, 14

$V \cdot cm^{-1}$, and 18 $V \cdot cm^{-1}$ respectively. Each funnel is supplied voltage from its own RF generator such that F1 receives 70 V_{p-p} (450 kHz), F2 receives 100 V_{p-p} (480 kHz), and F3 receives 70 V_{p-p} (450 kHz). By raising a positive potential at the first lens, these funnels are capable of gating the ion beam and can be used to select a small packet of ions similar in mobility. Ion activation and collision-induced dissociation can be introduced inside the funnels to alter the population of transmitted ions. The ferocity of these collisions can be controlled by changing the voltage drop at the end of the funnel. Utilizing these abilities at F2 divides the total drift tube length (~181 cm) into two separate drift regions, D1 (87.1 cm) and D2 (94.9 cm), which is tantamount to two-dimensional IMS. An orthogonal reflectron TOFMS provides a nested drift(flight) time measurement used to calculate both m/z and drift time.

Sample preparation and electrospray conditions

The three dipeptides RA, LN, and KV were synthesized in-house via routine solid phase synthesis (SPS) techniques. The specific SPS scheme used utilized Fmoc (fluroenylmethoxycarbonyl) chemistry and Wang resin polymer beads (Nova Biochem). These beads came preloaded with one amino acid of choice already tethered to the bead. After swelling the beads in DMF, the tethered peptides were deprotected by removing the Fmoc groups using 20% (v/v) piperidine in DMF. After thorough rinsing, a coupling solution was added containing 4 equivalents of the next Fmoc-protected amino acid to be added, along with 3.9 equivalents of 2-(1-H-Benzotriazol-1-yl-)-1,1,3,3-tetramethyluronium hexafluorophosphate (HBTU), and 4 equivalents of N-methylmorpholine in DMF. After a second deprotection, the dipeptides were cleaved from the solid-phase support using a standard cleavage cocktail of trifluoroacetic

acid/phenol/water/thioanisole/ethandithiol in 82.5:5:5:5:2.5 by volume. The filtrate containing the peptides was collected and the peptides were precipitated upon the addition of ether. After several washes with ether, the peptides were dissolved in 30% aqueous solution of acetic acid and lyophilized.

Horse heart cytochrome *c* was obtained from Sigma (>90% purity) and digested with trypsin. 15mg of protein was added to 3 mL of 2 M urea (in 0.2 M Tris(hydroxymethyl)aminomethane and 10 mM $CaCl_2$, pH 8) before being treated with 2% (w/w) TPCK-treated trypsin (Sigma) in 0.2 M Tris(hydroxymethyl)aminomethane, 10 mM $CaCl_2$ (pH 8). After 24 hours of digestion at 37 °C, the tryptic peptides were retrieved by C-18 Sep-Pak cartridge filtration (Waters), and purified by lyophilization. From this digest, a 0.25mg/mL sample was prepared in a 49:49:2 solution of water:acetonitrile:acetic acid.

A syringe pump (*kd* Scientific, Holliston, MA) was used to deliver sample at a flow rate of 0.25 $\mu L \cdot min^{-1}$ through a pulled capillary tip (75 μm i.d. × 360 μm o.d.) biased 2.2 kV above the drift voltage. The dipeptide solution used had a concentration of 1.5mM, while the cytochrome *c* digest was sprayed at 0.10mg/mL. To form the non-covalent complexes, 50 equivalents of 18-crown-6 ether (Aldrich, 99%) were added to the dipeptide solution and to a 0.25mg/mL cytochrome *c* digest solution. Data were typically collect for one minute for the solutions without crown ether, and for 5 minutes with the crown ether.

Results:

The experiments succeeded in showing reproducibility of the work on dipeptides. Preliminary results (Fig. 5) showed many of the same features as the previous data. The dipeptides became more resolved after the addition of crown ether, and while unintentionally fragmenting at the back of the drift tube, some parent peptides were observed at the same drift time as the dipeptide/crown complex. Even the complex featuring residual trifluoroacetate was seen.

In addition to the total spectrum, the use of an IMS-CID-IMS-MS instrument allowed the selection of only the dipeptide/18C6 complex (Fig. 6) followed by CID and an additional leg of IMS resolution. By varying the voltage drop across the CID region, one can tune the extent of the dissociation. Selecting several voltages, we were able to illustrate the increasing removal of 18C6 from the peptide until the complex was virtually eliminated (Figs. 7&8). Even more energetic collisions were able to induce fragmentation of the peptide at the same time as adduct removal (Fig9). A stack plot of the mass spectra for this drift time selection is also supplied for a simplified figure (Fig. 10).

After achieving reproducible results on a higher-resolution instrument which matched those from experiments conducted previously by others, this technique was ready to be applied to a significantly more complex sample. Tables 2 and 3 show all of the identified peaks from these experiments. Table 2 lists the observed tryptic peptides, labeled alphabetically in increasing neutral mass, preceded by a number which represents its charge state. Table 3 shows the peptides observed when sprayed with 18C6, as well as the complexes they form. These assignments must include an additional parameter to distinguish between the variable addition of 18C6 adducts to that peptide. To this end, an additional number representative of the 18C6 adducts was added to the previously

mentioned label. These labels were then used in Figure 11, showing the IMS-MS spectrum of the digest sprayed alone (a) and with 18C6 (b).

The addition of crown ether to the sample produced some interesting and wide-sweeping results. It may be expected that the addition of crown ether to a protonated amine would serve to stabilize the excess charge by coordinating to the numerous oxygen atoms in the polyether. This resulted in increased ionization efficiency of the electrospray source, which in turn increased signal beyond the expected gains due to increased concentration and acquisition times. The stabilization of charge also made several higher charge states of the peptides accessible. In general, peptides were able to support one extra charge upon the addition of 18C6.

Three peptides were only observed when sprayed in the presence of 18C6. Interestingly, all of these peptides, EETLMEYLENPKK, YIPGTKMIFAGIK, and GGKHK, are tryptic miscleaveages. Peptides EETLMEYLENPKK and GGKHK both contain lysine residues very close together in the sequence. If both lysine residues are protonated during ionization, these residues would experience columbic repulsion and possibly dissociate. Seemingly, these peptides are stable ions only when 18C6 is present to support or shield the excess charge. This explanation, however, fails to encompass the absence of YIPGTKMIFAGIK. The separation of these lysine residues should minimize the repulsions between the positive side-chains. The presence of IFVQKCAQCHTVEK, another miscleaveage, without 18C6 demonstrates the stabilization provided by sufficient separation of the lysine residues. YIPGTK and MIFAGIK, however, are the only evidence of YIPGTKMIFAGIK in the absence of 18C6. The reason for the instability of this miscleaveage remains debatable and would require further experiments to resolve.

Figures 12 and 13 display spectra of selections taken at two different mobilities that were subsequently energized at two different intensities. CID at 125.7 V generally proved sufficient to remove at least one 18C6 adduct from the selected complexes, while 165.7 V usually retrieved at least some portion of the parent peptide. At this extreme, CID also caused charge transfer, made evident by the appearance of 2m0. As shown in Figure 13, 165.7 V also proved sufficient to produce fragmentation of IFVQKCAQCHTVEK into IFVQK. As a result of all these processes, the composition of the selected packet of ions changes significantly. While each component had similar mobility during the first IMS separation, these alterations produces a population of ions that are resolvable in the second dimension of IMS. One peculiar result of this second phase of separation is the appearance of a +4 ion in a line of +3 ions. Because IMS usually separates ions into families of charge states, a +4 ion displaying a mobility lower than that of +3 ions, including the +3 charge state of itself, initially seems perplexing. This oddity was made possible by the addition of two 18C6 adducts to the +4 ion. This increase in collision cross-section caused a subsequent decrease in mobility slightly more potent than the reduction in mobility that would result from the removal of one charge from the peptide ion.

This observation warranted a more precise definition of the effect these adducts have on the mobility of various peptides. Obviously, increasing the number of 18C6 adducts to a peptide will continually increase its collision-cross section. What is not initially apparent, however, is if the impact per adduct diminishes upon further additions of 18C6 or upon addition to increasingly larger peptides. Figure 14 depicts a graphical attempt at answering this question. The graphs group the ions into +2 and +3 charge state

families and plot the drift time of the naked peptide against the drift time of its complexes with 18C6. Each vertical line of points therefore comes from the same peptide, and each point represents a complex of the same peptide with a different number of 18C6 adducts. In this way, one could observe the additive effect of increasing the number of adducts on a given peptide. Additionally, the effect of a given number of 18C6 adducts could be visualized as the size of the peptide varied. It was expected that a size cut-off existed, after which the addition of one 18C6 adduct to a peptide no longer produced a significant change in mobility, thereby limiting the usefulness of this separation technique on large peptides. This point would therefore lie on the diagonal line y = x. Therefore, by extrapolating the best-fit line of each series to its intersection with y = x, one can predict the cut-off drift time. As expected, these best-fit lines intersect with the y = x line, and fortunately for the application of this technique, at drift times much greater than that of any species observed in these studies (~80 ms and ~250 ms for the plot of +2 ions and +3 ions respectively). For the plot of +3 ions, the best-fit lines intersected with y = x in the anticipated order; single additions of 18C6 intersected at the shortest drift time, and quadruple additions of 18C6 intersected at the longest drift time. The +2 ions, however, displayed the exact opposite trend. Furthermore, this finding is made even increasingly troublesome taking into account that the number of data points suggests the trend given by the plot of +2 ions is more trustworthy. Clearly, some flaw is present in the hypothesis outlined above which requires future work.

The results of the experiment clearly demonstrate the abilities of this particular technique, even if a few discontinuities with the initial expectations still exist. Although these data have not yet been assimilated into an adjusted explanatory theory, progressing

into further studies may shed light on additional helpful insights on resolving the differences between the hypothesis and the data.

Future Work:

Glu-C Digest

The tryptic digest made an excellent proof-of-principle experiment for many reasons. These digests readily provide complex mixtures and are highly relevant to characterizing biological samples. Perhaps most importantly, however, by cleaving a protein into segments at lysine or arginine residues, every tryptic peptide has at least one basic residue in addition to its N-terminus. While the tryptic digest ensures a target for 18C6 on every peptide, this property can also be viewed as a correlation which limits resolving power. Every peptide might be expected to have the same number of adducts, and the result may simply be separation on the basis of the number of miscleaveages in the peptides. A future experiment could be to perform a Glu-C digest on the same protein as before and analyze it with crown ether. A Glu-C digest cleaves proteins at acidic residues, leaving room for the basic residues per peptide to vary as it may, effectively eliminating the correlations inherent to a tryptic digest.

Non-covalent Labeling

The use of covalent modifications and isotope markers as labels in protein analysis has proven to be a tremendously useful technique[17]. If a non-covalent complex were used as the label, however, the method would be further improved in the sense that the complex could be dissociated to retrieve the parent peptide. With that consideration in mind, deuterated crown ether presents an interesting possibility. In the case of 18C6, a

deuterated analog would provide a convenient neutral mass shift of 24 Da, which divides into an integer for +2, +3, and +4 charge states. In addition, the specificity of 18C6 has been well characterized. Presumably, 18C6 and deuterated 18C6 could be used to label two samples prior to combination for high through-put analysis. Future work in this project primarily entails studying the robustness of the technique, such as addressing if the extent of H/D exchange or dynamic equilibrium will interfere with the interpretation of the results.

Acknowledgements:

I would like to thank Prof. David Clemmer for allowing me to conduct research in his group for the first year of my graduate career. I would also like to thank all the members of the Clemmer Group for their support and assistance, especially Stormy Koeniger and Samuel Merenbloom, as they have worked with me most directly. Special thanks to Amy Hilderbrand for her valuable resources and initial work on this project.

References

1. Hill, H. H.; Siems, W. F.; St. Louis, R. H.; McMinn, D. G. *Anal. Chem.* **1997**, *62*, A1201- A1209.

2. Hoaglund-Hyzer, C. S.; Lee, Y. J.; Counterman, A. E.; Clemmer, D. E. *Anal. Chem.* **2002**, *74*, 992-1006.

3. von Helden, G.; Wyttenbach, T.; Bowers, M. T. *Science*. **1995**, *267*, 1483.

4. Hoaglund, C. S.; Valentine, S. J.; Sporleder, C. R.; Reilly, J. P.; Clemmer, D. E. *Anal. Chem*. **1998**, *70*, 2236-2242.

5. Jarrold, M. F. *J. Phys. Chem.* **1995**, *99*, 11.

6. Wyttenbach, T.; von Helden, G.; Bowers, M. T. *J. Am. Chem. Soc*. **1996**, *118*, 8355.

7. Clemmer, D. E.; Hudgins, R. R.; Jarrold, M. F. *J. Am. Chem. Soc*. **1995**, *117*, 10141.

8. Clemmer, D.E.; Jarrold, M. F. *J. Mass. Spectrom.* **1997**, *32*, 577-592.

9. von Helden, G.; Wyttenbach, T.; Bowers, M. T. *Int. J. Mass. Spectrom. Ion Processes*. **1995**, *146/147*, 349.

10. Lee, Y. J.; Hoaglund-Hyzer, C. S.; Srebalus Barnes, C. A.; Hilderbrand, A. E.; Valentine, S. J.; Clemmer, D. E. *J. Chromatography B*. **2002**, *782*, 343-351.

11. Valentine, S. J.; Koeniger, S. L.; Clemmer, D. E. *Anal. Chem.* **2003**, *75*, 6202-6208.

12. Koeniger, S. L.; Merenbloom, S. I.; Valentine, S. J.; Jarrold, M. F.; Udseth, H.; Smith, R.; Clemmer, D. E. *Anal. Chem*. (submitted 06/05, accepted 03/06)

13. Julian, R.R; Beauchamp, J.L. *Int. J. Mass Spectrom*. **2001**, *210/211*, 613-623.

14. Colgrave ML, Bramwell CJ, Creaser CS. *Int. J. Mass Spec*, **2003**, 229, 209-216

15. Hilderbrand, A. E.; Myung, S.; Srebalus Barnes, C. A.; Clemmer, D. E. *J. Am. Soc. Mass. Spectrom.* **2003**, *14*, 1424-1436.

16. Hilderbrand, A.E; Chapter 7 of Ph.D Thesis. Indiana University. 2005

17. Beardsley, R. L.; Sharon, L. A.; Reilly, J. P. *Anal. Chem.* in press (2005).

Captions for Tables and Figures

Table 1: Comparision of collisional cross section (in $Å^2$) and mobility (in $cm^2V^{-1}s^{-1}$) between two tetrapeptides. M denotes monomer peptide unit. The dimer's properties have been shown for reference.

Figure 1: IMS-MS spectrum of a tripeptide library before the addition of crown ether.

Figure 2: IMS-MS spectrum of a tripeptide library after the addition of crown ether. From left to right, one can see the remaining uncomplexed tripeptides, the tripeptides complexed to one equivalent of 18C6, and the tripeptides complexed to two equivalents of 18C6 as well as one equivalent of trifluroacetate remaining from the library synthesis.

Figure 3: IMS-MS spectrum after the removal of 18C6 at the back of the drift tube. The parent peptides are retrieved, but appear at the drift times as their respective complexes.

Fig. 4: Schematic diagram of the IMS-CID-IMS-TOFMS instrument uniquely suited to perform the study of noncovalent complexes. This home-built instrument consists of two drift regions nearly equal in length separated by an ion funnel which can be used to improve ion transmission as well as provide collision-induced dissociation. The drift tube then leads to a reflectron time-of-flight mass spectrometer for mass analysis.

Figure 5: IMS-MS spectrum showing the shift in mobility of three dipeptides (RA, LN, and KV). Unintentional fragmentation at the back of the drift tube actually serves to show the parent peptide at the mobility-shifted drift time.

Figure 6: Drift-time selection of the dipeptide/18C6 complex. The mobility of the dipeptide's dimer is similar enough to the complex to appear at low intensity in this selection. The selection was made halfway through the drift tube between 7.5 and 7.6ms, meaning ions with drift times of around 15ms throughout the drift tube are observed.

Figure 7: CID of the dipeptide/18C6 complex at the middle of the drift tube using an excitation voltage of 147.5 V shows partial removal of the 18C6. During the second IMS stage of the instrument, the smaller peptide moves ahead of the complex in drift time.

Figure 8: Increasingly energetic collisions results in more efficient removal of the 18C6 adduct from the peptide.

Figure 9: At sufficiently high energy, the 18C6 is completely removed and the dipeptide begins to fragment, allowing the single residues to resolve in drift time.

Figure 10: Mass spectra of the dipeptide/ether mixture from each CID experiment stacked over one another for easy and direct comparison.

Table 2: This table displays all of the tryptic peptides observed in the IMS-MS spectrum when sprayed without 18C6. Empty rows have been included for peptides observed only in the presence of 18C6.

Table 3: This table lists all peptides and peptide/18C6 complexes observed when the digest and 18C6 are sprayed together. Because of the variability in the number of 18C6 adducts to a given peptide with a given charge state, the table had to be divided into charge state families.

Figure 11: Two nested drift(flight) time plots for a tryptic digest of horse cytochrome *c* (0.25mg/mL) sprayed alone (a) and with 18-crown-6 ether (b). Diagonal lines depicting the general location of the observed charge states are labeled on each graph. The two vertical lines on (b) show the selections made later in the experiment. The labels on the spectra are referenced to a specific peptide in a given charge state with varying numbers of crown ether adducts, which can be found in Table 1. The first number corresponds to the charge state, the letter was alphabetically assigned to the observed peptides in order of increasing m/z, and the second number distinguishes the number of crown ether adducts associated to the peptide.

Figure 12: A selected packet of ions with total drift times in the range of 15.52-15.73ms is transmitted with no activation (a), with IA2=125.7V (b), and with IA2=165.7V (c). As collisions in IA2 become more energetic, one can observe the stepwise loss of 18-crown-6 ether adducts from complex.

Figure 13: A selected packet of ions with total drift times in the range of 13.65-13.85ms is transmitted with no activation (a), with IA2=125.7V (b), and with IA2=165.7V (c). Demonstrated here is the ability to control the selection's position in drift time, as well as the tunable extent of dissociation.

Figure 14: A plot comparing the drift time of an uncomplexed peptide to its drift time with the addition of one or several 18-crown-6 ether adducts. A diagonal line resulting from plotting the original drift time against itself is shown for reference.

Table 1

Polyether	MRFA		MFAR		Difference	
	K_0	Ω_D	K_0	Ω_D	ΔK_0	$\Delta\Omega_D$
Free	1.495	124.4	1.478	125.8	0.017	-1.4
M+12C4	1.32	139.9	1.314	140.6	0.006	-0.7
M+T3G	1.322	139.7	1.313	140.7	0.009	-1
M+15C5	1.294	142.6	1.29	143	0.004	-0.4
M+T4G	1.291	142.9	1.285	143.6	0.006	-0.7
M+18C6	1.27	145.1	1.267	145.5	0.003	-0.4

Polyether	MRFA		MFAR		Difference	
	K_0	Ω_D	K_0	Ω_D	ΔK_0	$\Delta\Omega_D$
Dimer	0.906	202.6	0.893	205.5	0.013	-2.9
$M+(12C4)_2$	N/A	N/A	1.144	160.8	N/A	N/A
$M+(T3G)_2$	1.166	157.8	1.13	162.8	0.036	-5
$M+(15C5)_2$	1.131	162.5	1.099	167.2	0.032	-4.7
$M+(T4G)_2$	1.118	164.3	1.08	170.1	0.038	-5.8
$M+(18C6)_2$	1.089	168.5	1.057	173.6	0.032	-5.1

Figure 1

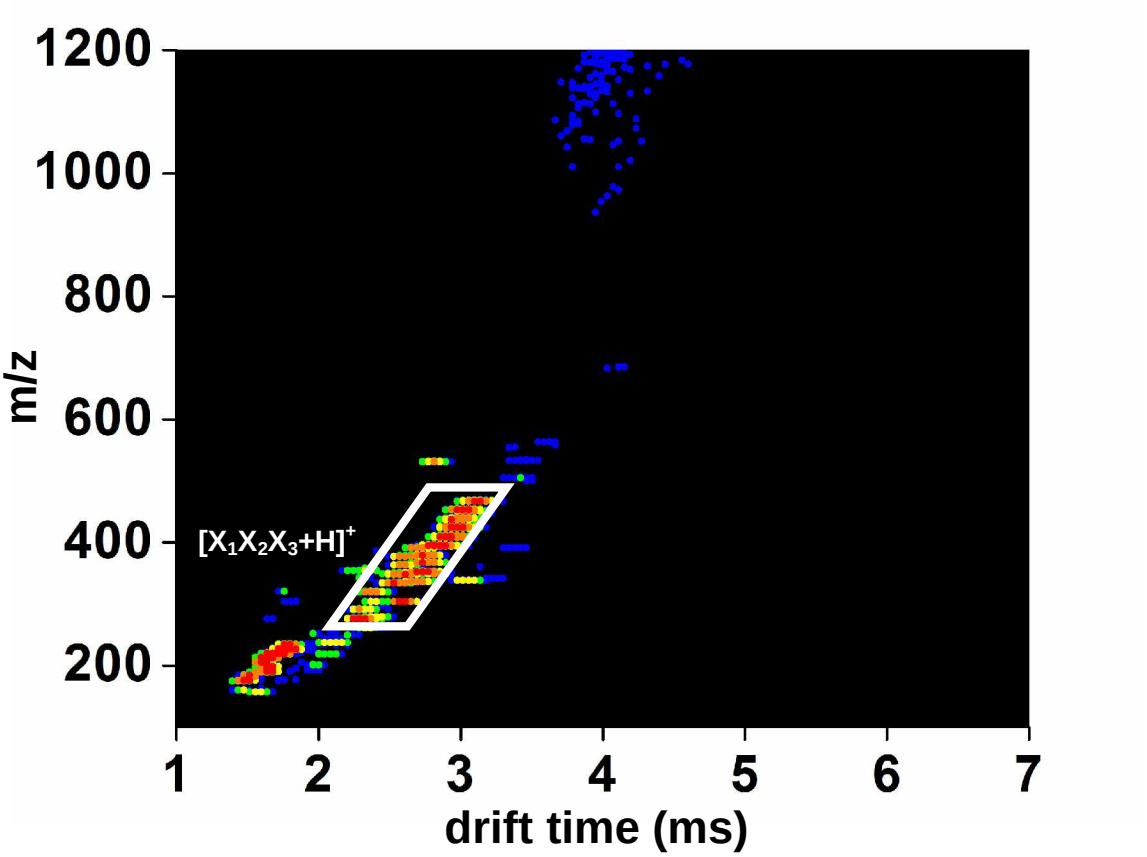

Figure 2

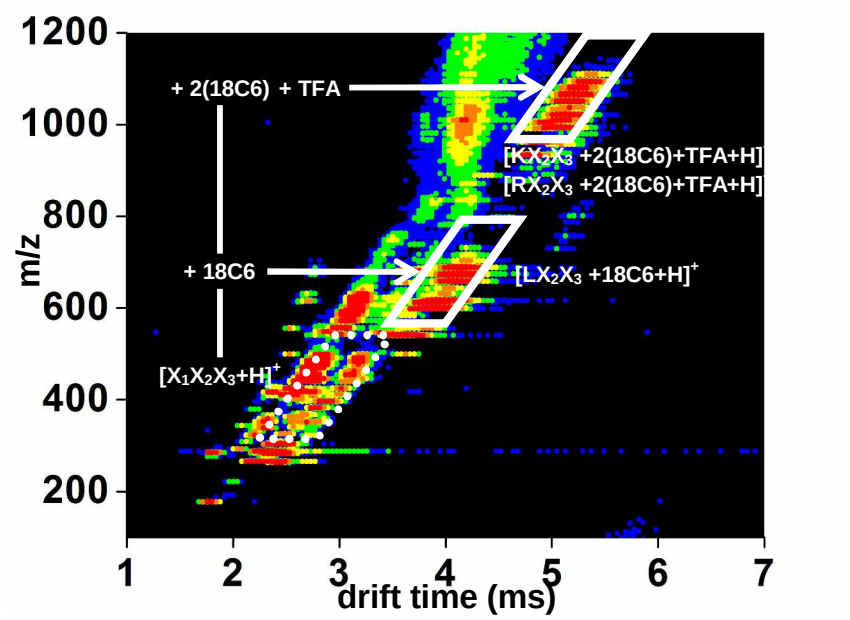

.

Figure 3

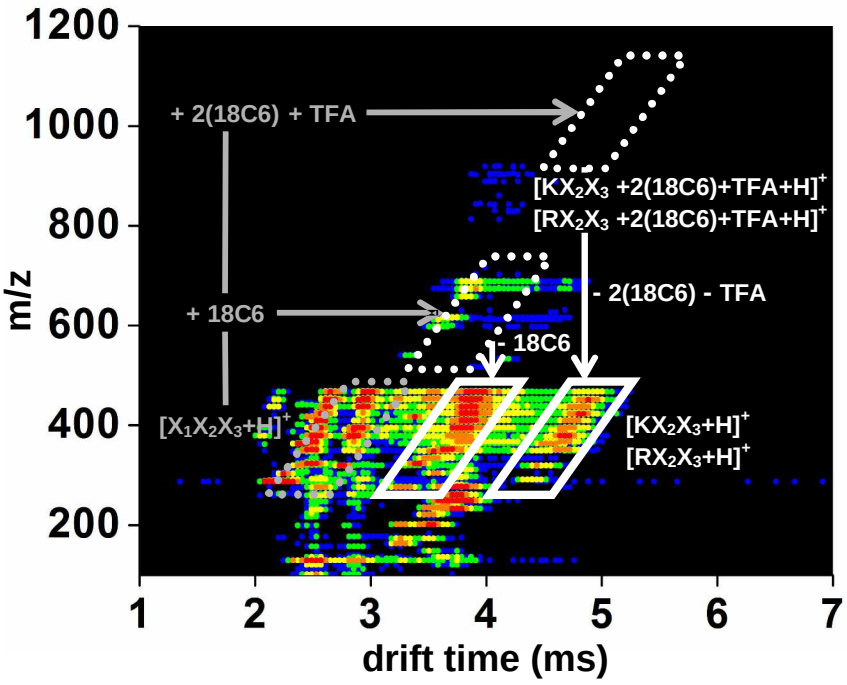

Figure 4

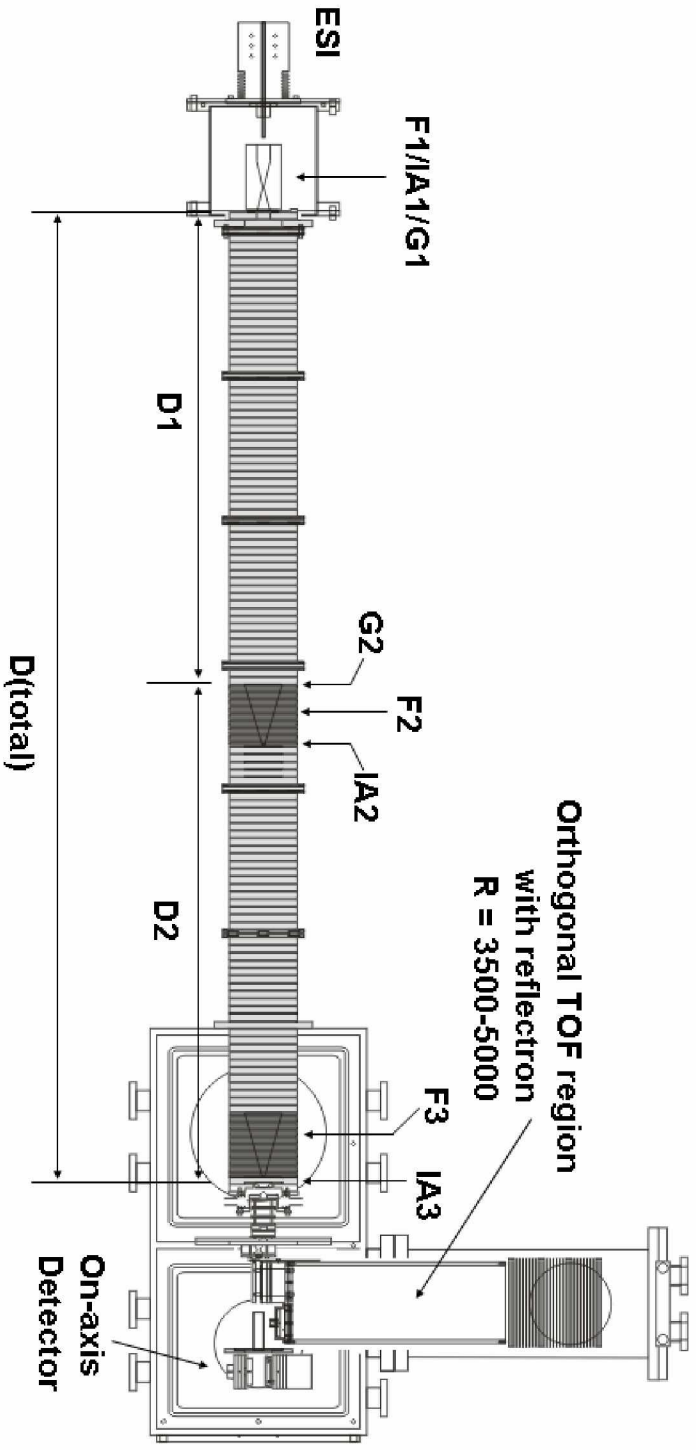
ESI
F1/IA1/G1
D1
D(total)
G2
F2
IA2
D2
Orthogonal TOF region
with reflectron
R = 3500-5000
F3
IA3
On-axis
Detector

Figure 5

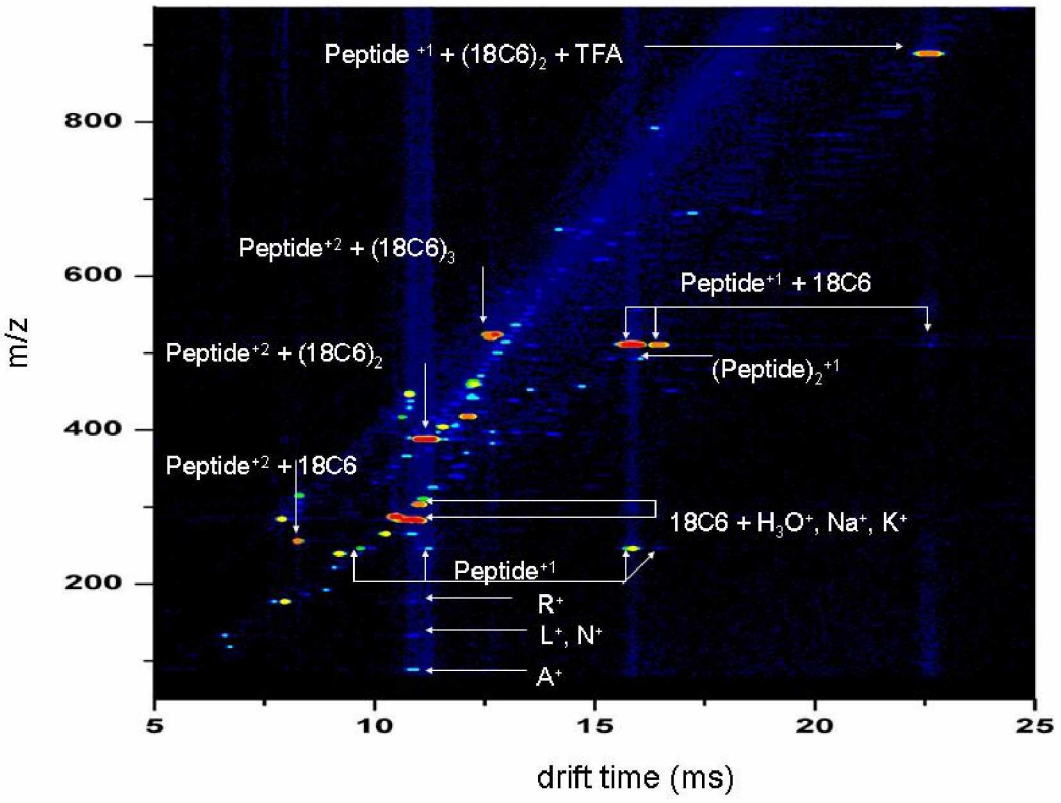
Peptide +1 + (18C6)2 + TFA
Peptide+2 + (18C6)3
Peptide+1 + 18C6
Peptide+2 + (18C6)2
(Peptide)2+1
Peptide+2 + 18C6
18C6 + H3O+, Na+, K+
Peptide+1
R+
L+, N+
A+
m/z
800
600
400
200
5
10
15
20
25
drift time (ms)

Figure 6

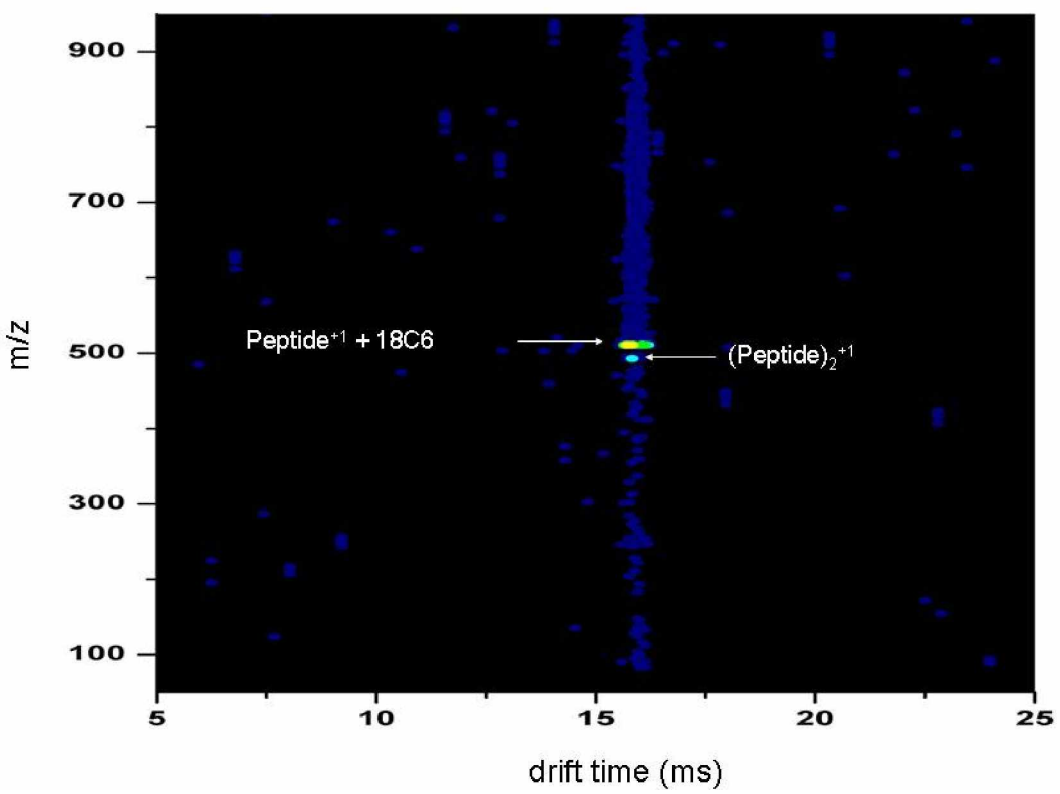
900
700
500
300
100
m/z
Peptide+1 + 18C6
(Peptide)2+1
5
10
15
20
25
drift time (ms)

Figure 7

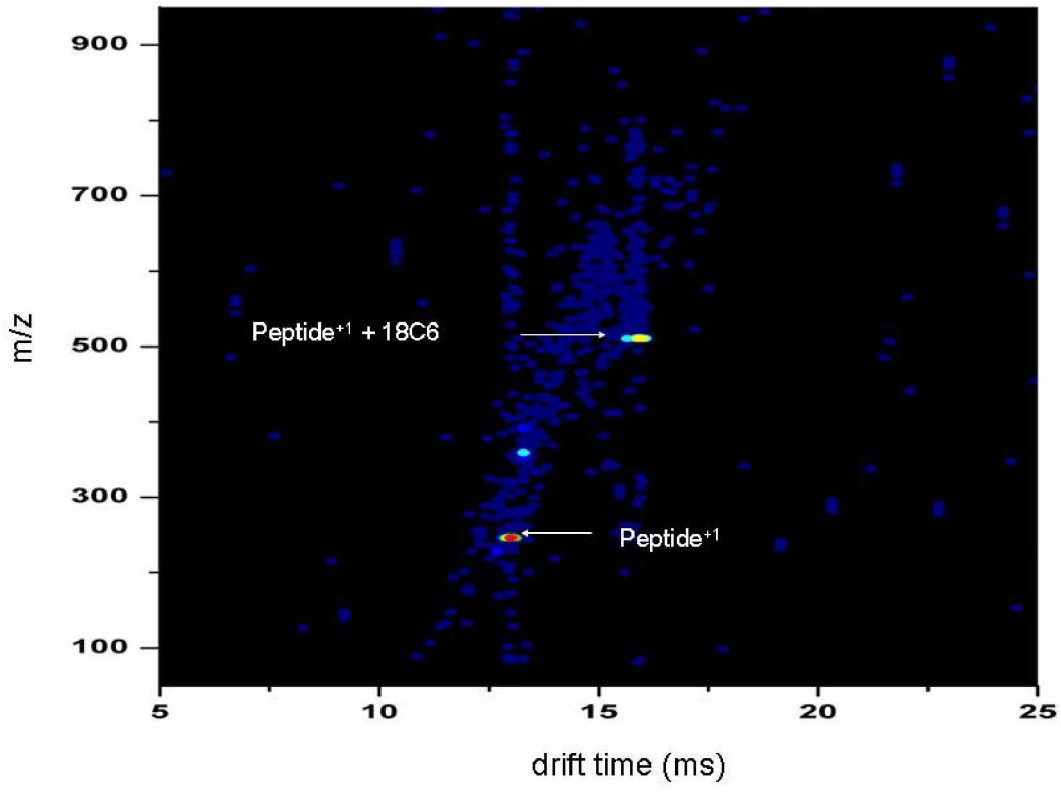
900
700
500
300
100
m/z
Peptide+1 + 18C6
Peptide+1
5
10
15
20
25
drift time (ms)

Figure 8

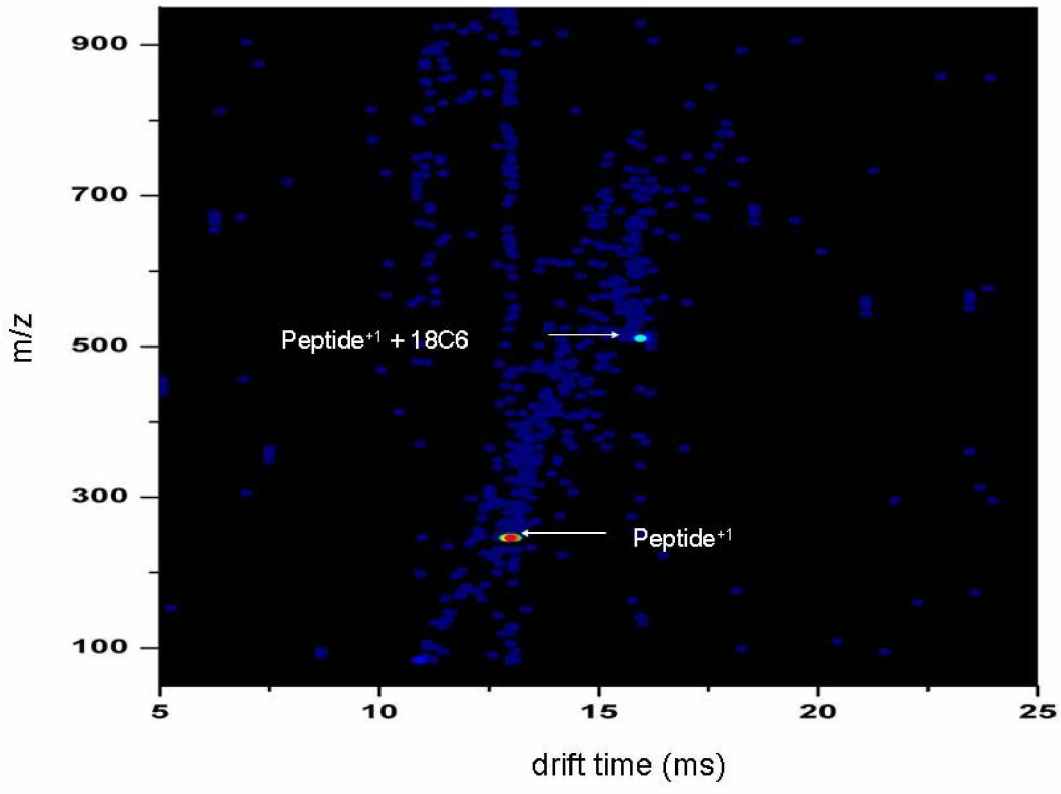
900
700
500
300
100
m/z
Peptide+1 + 18C6
Peptide+1
5
10
15
20
25
drift time (ms)

Figure 9

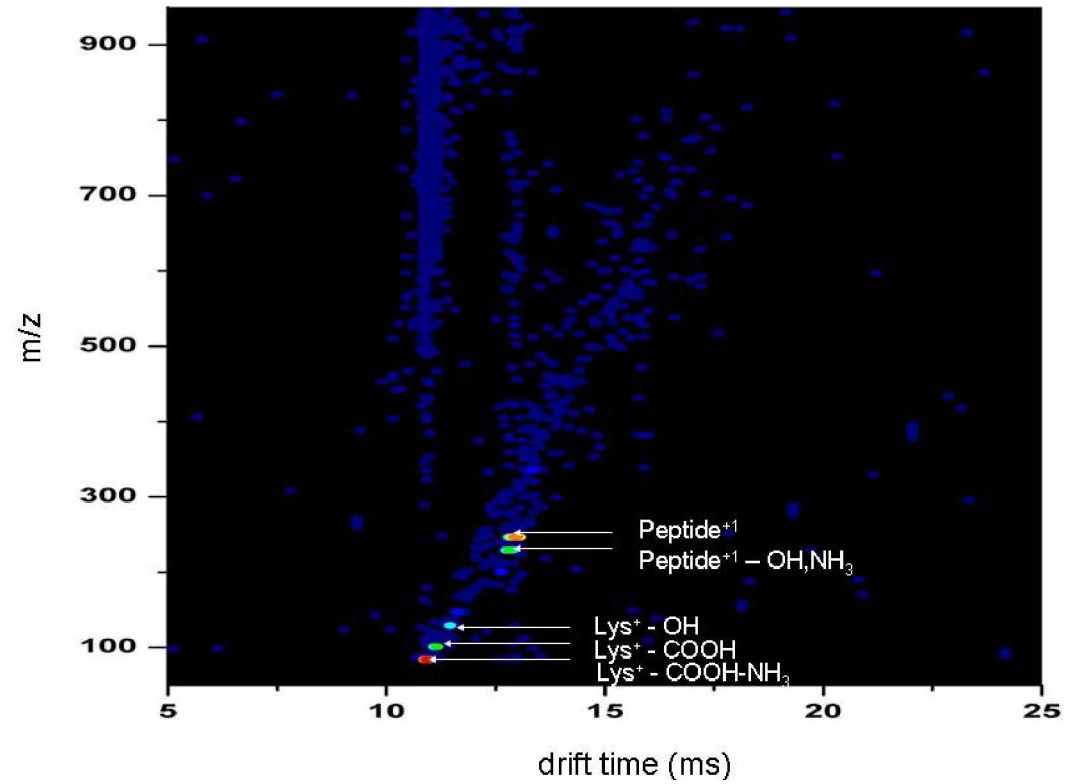
900
700
500
300
100
m/z
5
10
15
20
25
drift time (ms)
Peptide+1
Peptide+1 – OH,NH3
Lys+ - OH
Lys+ - COOH
Lys+ - COOH-NH3

Figure 10

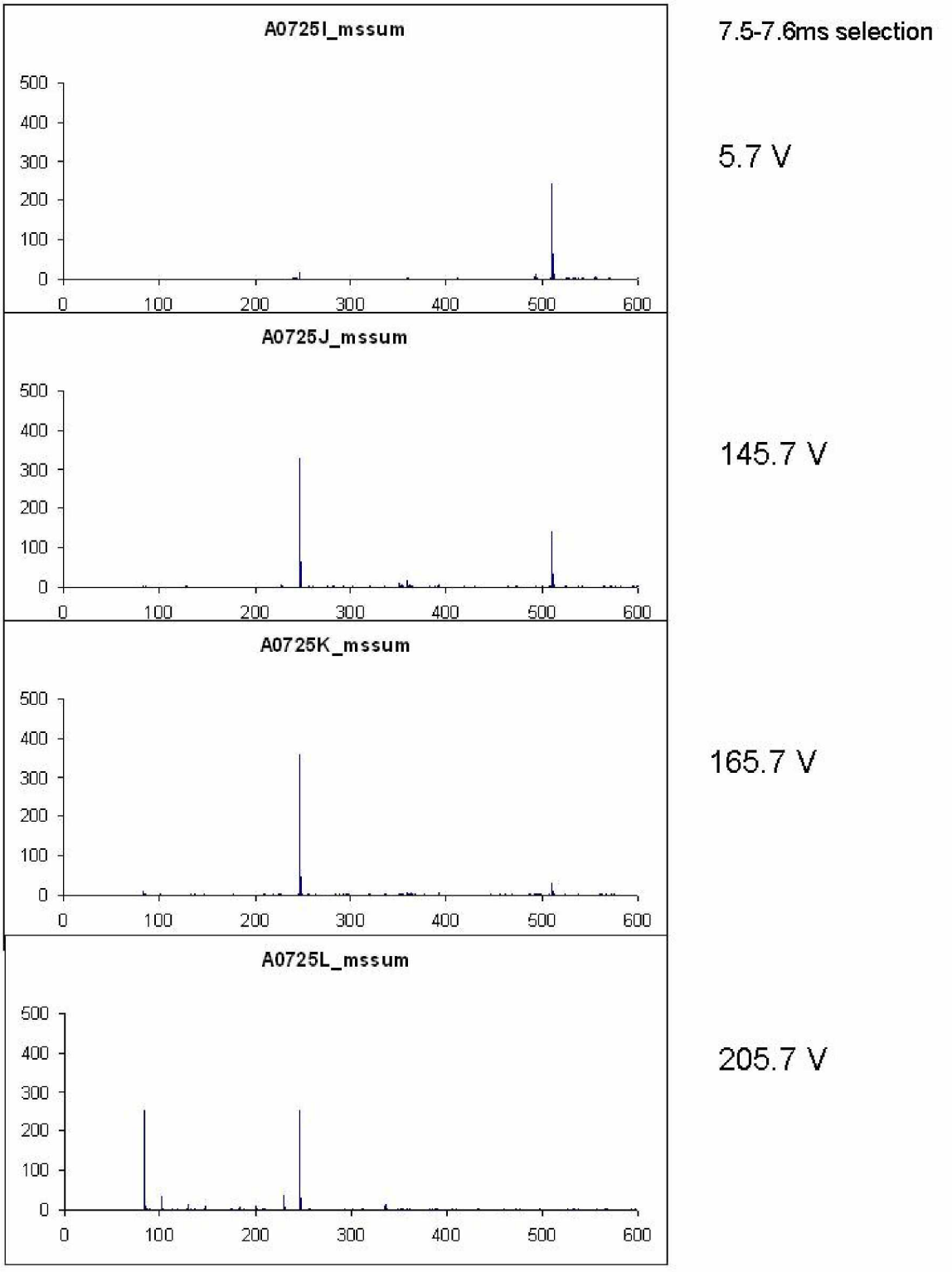
A0725I_mssum
A0725J_mssum
A0725K_mssum
A0725L_mssum
0
100
200
300
400
500
600
7.5-7.6ms selection
5.7 V
145.7 V
165.7 V
205.7 V

Table 2

Without Crown			**Plus Ones**	**Plus Twos**	**Plus Threes**
		neutral mass	**Label (m/z)**	**Label (m/z)**	**Label (m/z)**
IFVQKCAQCHTVEK	m	1632.8109			3m (545.3)
EETLMEYLENPKK	l	1622.7854			
KTGQAPGFTYTDANK	k	1597.7729			3k (533.6)
EETLMEYLENPK	j	1494.6905		2j (748.3)	
TGQAPGFTYTDANK	i	1469.6779		2i (735.8)	
YIPGTKMIFAGIK	h	1437.8046			
TGPNLHGLFGR	g	1167.6141		2g (584.8)	
KYIPGTK	f	805.469		2f (403.7)	
MIFAGIK	e	778.4404	1e (779.4)	2e (390.2)	
YIPGTK	d	677.3741	1d (678.4)	2d (339.7)	
IFVQK	c	633.3842	1c (634.4)	2c (317.7)	
GITWK	b	603.3373	1b (604.3)	2b (302.8)	
GGKHK	a	525.3016			

Table 3

With Crown			**Plus Ones**	**Plus Twos**			
		neutral mass	**Label (m/z)**	**Label (m/z)**	**1crown**	**2crown**	**3crown**
IFVQKCAQCHTVEK	m	1632.8109					
EETLMEYLENPKK	l	1622.7854					
KTGQAPGFTYTDANK	k	1597.7729					
EETLMEYLENPK	j	1494.6905		2j0 (748.3)	2j1 (880.4)		
TGQAPGFTYTDANK	i	1469.6779			2i1 (867.9)		
YIPGTKMIFAGIK	h	1437.8046					
TGPNLHGLFGR	g	1167.6141					
KYIPGTK	f	805.469			2f1 (535.8)		
MIFAGIK	e	778.4404			2e1 (522.3)	2e2 (654.4)	2e3 (786.5)
YIPGTK	d	677.3741		2d0 (339.7)	2d1 (471.8)	2d2 (603.8)	2d3 (735.9)
IFVQK	c	633.3842		2c0 (317.7)	2c1 (449.8)	2c2 (571.9)	
GITWK	b	603.3373		2b0 (302.6)	2b1 (434.7)	2b2 (566.8)	
GGKHK	a	525.3016			2a1 (395.7)		
With Crown			**Plus Threes**				
		neutral mass	**Label (m/z)**	**1crown**	**2crown**	**3crown**	**4crown**
IFVQKCAQCHTVEK	m	1632.8109		3m1 (633.3)	3m2 (721.4)	3m3 (809.4)	
EETLMEYLENPKK	l	1622.7854			3l2 (718.0)	3l3 (806.1)	
KTGQAPGFTYTDANK	k	1597.7729	3k0 (533.6)	3k1 (621.6)	3k2 (709.7)		
EETLMEYLENPK	j	1494.6905		3j1 (587.3)	3j2 (675.3)		
TGQAPGFTYTDANK	i	1469.6779					
YIPGTKMIFAGIK	h	1437.8046		3h1 (568.3)			
TGPNLHGLFGR	g	1167.6141		3g1 (478.3)	3g2 (566.3)	3g3 (654.4)	3g4 (742.4)
KYIPGTK	f	805.469					

MIFAGIK	e	778.4404					
YIPGTK	d	677.3741					
IFVQK	c	633.3842					
GITWK	b	603.3373					
GGKHK	a	525.3016					
With Crown			**Plus Fours**				
		neutral mass	**Label**	**1crown**	**2crown**	**3crown**	**4crown**
IFVQKCAQCHTVEK	m	1632.8109		4m1 (475.2)	4m2 (541.3)		

Figure 11

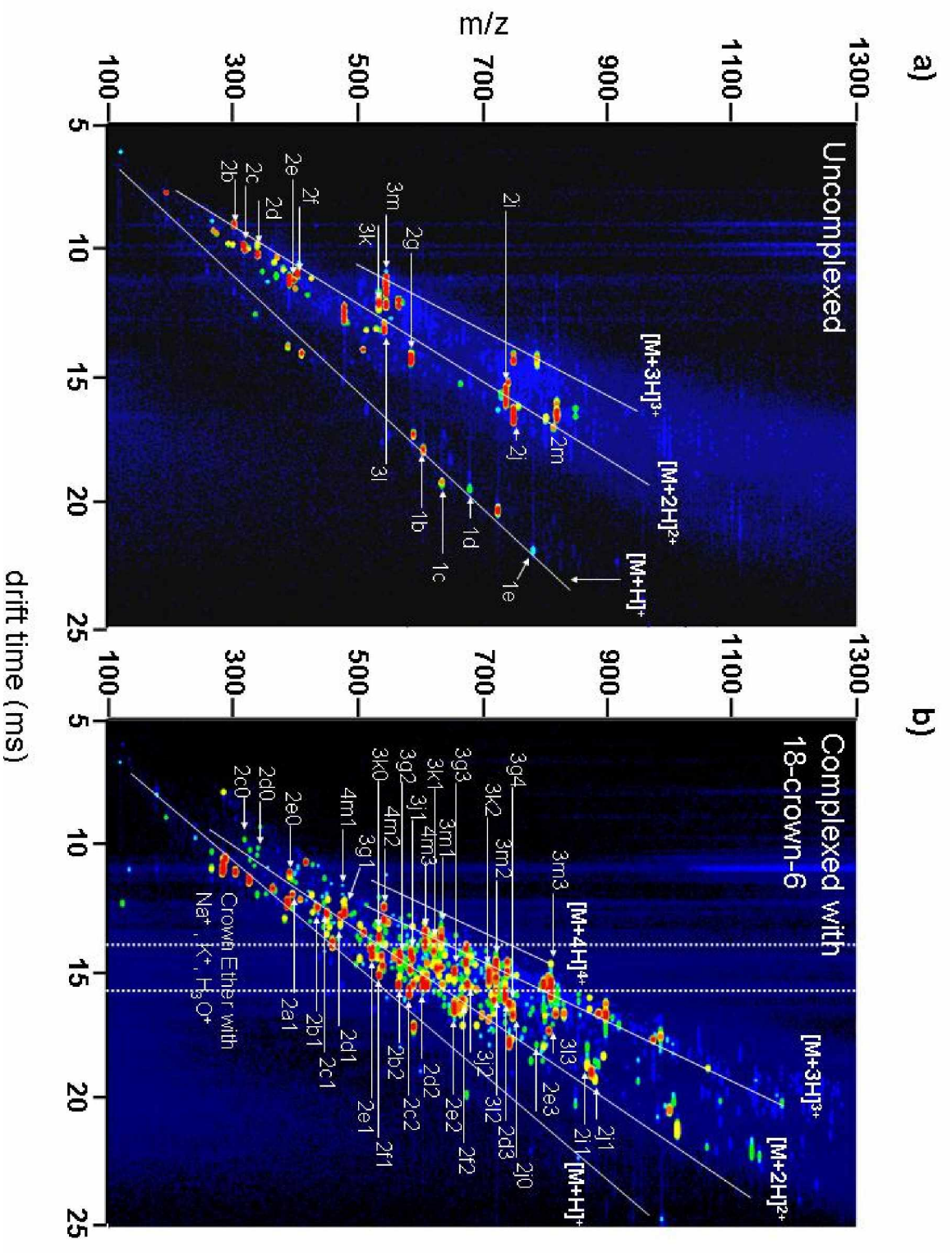
a)
Uncomplexed
[M+3H]3+
[M+2H]2+
[M+H]+
2i
2j
2m
1e
1d
1c
1b
3l
3k
3m
2g
2f
2e
2d
2c
2b
b)
Complexed with
18-crown-6
[M+3H]3+
[M+2H]2+
[M+4H]4+
[M+H]+
2j1
2i1
3l3
2e3
3m3
3g4
3k2
3m2
3g3
3m1
3k1
4m3
3j1
3g2
4m2
3k0
4m1
3g1
3j2
3l2
2d3
2j0
2e2
2f2
2d2
2c2
2b2
2e1
2f1
2d1
2c1
2b1
2a1
2e0
2d0
2c0
Crown Ether with
Na+, K+, H3O+
m/z
drift time (ms)
100
300
500
700
900
1100
1300
5
10
15
20
25

Figure 12

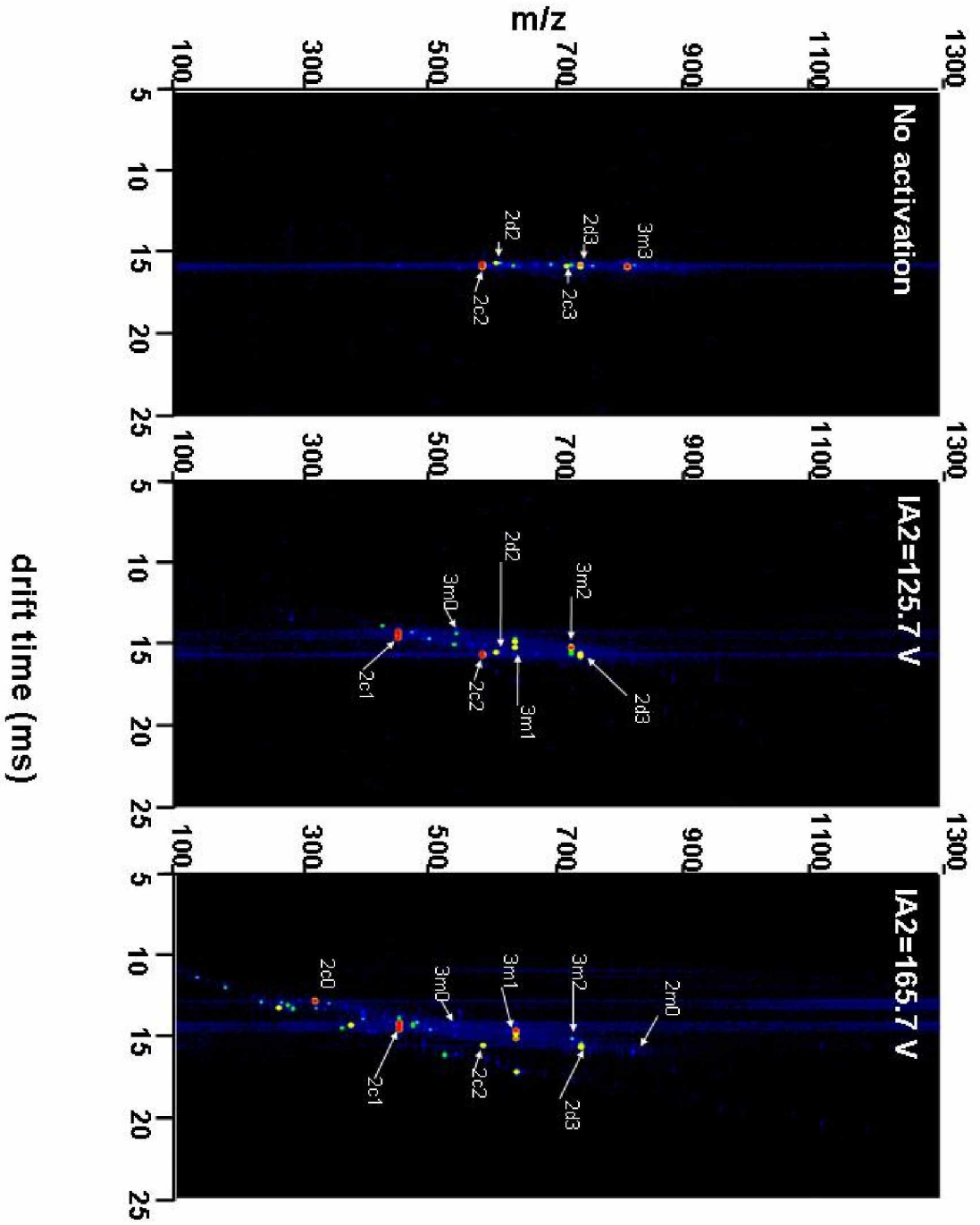
m/z
100
300
500
700
900
1100
1300
drift time (ms)
5
10
15
20
25
No activation
2d2
2d3
3m3
2c2
2c3
IA2=125.7 V
2d2
3m2
3m0
2c1
2c2
3m1
2d3
IA2=165.7 V
2c0
3m0
3m1
3m2
2m0
2c1
2c2
2d3

Figure 13

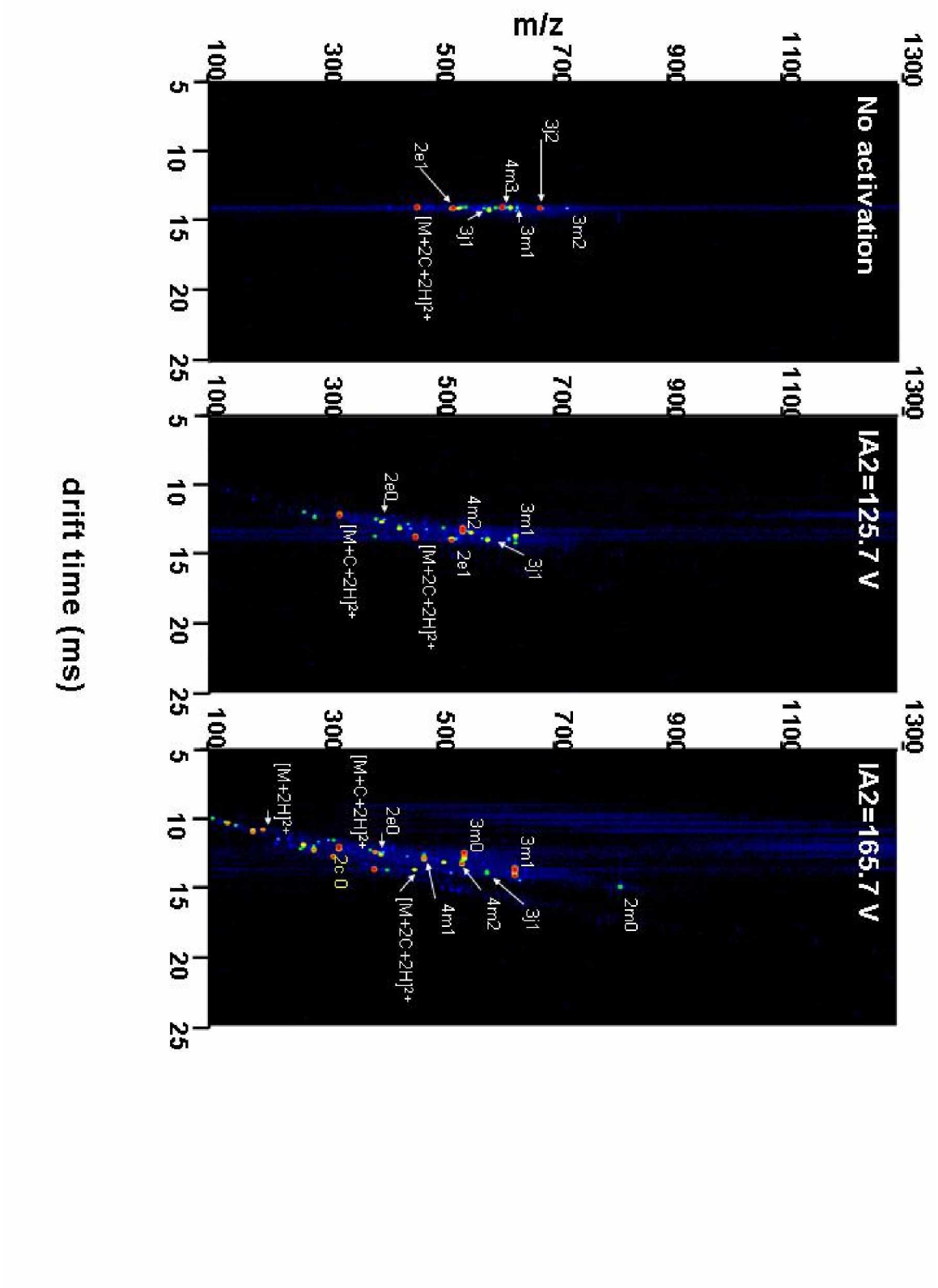
m/z
drift time (ms)
No activation
IA2=125.7 V
IA2=165.7 V
3j2
4m3
2e1
3m2
3m1
3j1
[M+2C+2H]2+
2e0
4m2
[M+C+2H]2+
[M+2H]2+
2c 0
3m0
4m1
2m0

Figure 14

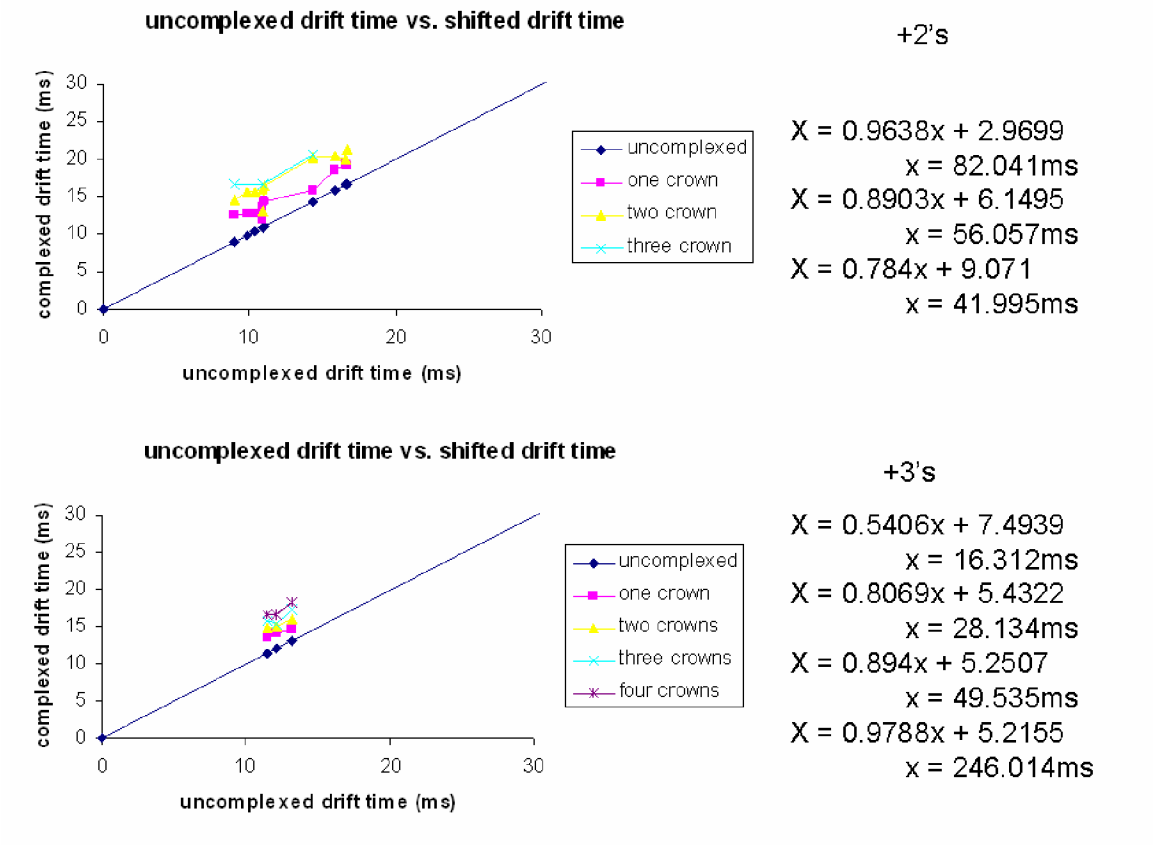
uncomplexed drift time vs. shifted drift time
complexed drift time (ms)
uncomplexed drift time (ms)
uncomplexed
one crown
two crown
three crown
+2's
X = 0.9638x + 2.9699
x = 82.041ms
X = 0.8903x + 6.1495
x = 56.057ms
X = 0.784x + 9.071
x = 41.995ms
uncomplexed drift time vs. shifted drift time
complexed drift time (ms)
uncomplexed drift time (ms)
uncomplexed
one crown
two crowns
three crowns
four crowns
+3's
X = 0.5406x + 7.4939
x = 16.312ms
X = 0.8069x + 5.4322
x = 28.134ms
X = 0.894x + 5.2507
x = 49.535ms
X = 0.9788x + 5.2155
x = 246.014ms